

Introducing a 2-His-1-Glu Nonheme Iron Center into Myoglobin Confers Nitric Oxide Reductase Activity

Ying-Wu Lin,^{†,‡} Natasha Yeung,[†] Yi-Gui Gao,[‡] Kyle D. Miner,[§] Lanyu Lei,[†] Howard Robinson,^{||} and Yi Lu^{*,†,§}

Department of Chemistry, George L. Clark X-ray Facility & 3M Materials Lab, Department of Biochemistry, University of Illinois at Urbana–Champaign, Urbana, Illinois 61801, and Department of Biology, Brookhaven National Laboratory, Upton, New York 11973

Received April 25, 2010; E-mail: yi-lu@illinois.edu

Abstract: A conserved 2-His-1-Glu metal center, as found in natural nonheme iron-containing enzymes, was engineered into sperm whale myoglobin by replacing Leu29 and Phe43 with Glu and His, respectively (swMb L29E, F43H, H64, called Fe_BMb(-His)). A high resolution (1.65 Å) crystal structure of Cu(II)-CN⁻-Fe_BMb(-His) was determined, demonstrating that the unique 2-His-1-Glu metal center was successfully created within swMb. The Fe_BMb(-His) can bind Cu, Fe, or Zn ions, with both Cu(I)-Fe_BMb(-His) and Fe(II)-Fe_BMb(-His) exhibiting nitric oxide reductase (NOR) activities. Cu dependent NOR activity was significantly higher than that of Fe in the same metal binding site. EPR studies showed that the reduction of NO to N₂O catalyzed by these two enzymes resulted in different intermediates; a five-coordinate heme-NO species was observed for Cu(I)-Fe_BMb(-His) due to the cleavage of the proximal heme Fe-His bond, while Fe(II)-Fe_BMb(-His) remained six-coordinate. Therefore, both the metal ligand, Glu29, and the metal itself, Cu or Fe, play crucial roles in NOR activity. This study presents a novel protein model of NOR and provides insights into a newly discovered member of the NOR family, gNOR.

Rational design of functional enzymes is a powerful strategy to gain deep insights into more complex native enzymes, as it is an ultimate test of our knowledge about the enzyme structure and function.¹ By conferring new activities, such an approach can reveal not only individual structural features necessary to contribute to the function of native enzymes, but also a set of structural features enough for the function. One such example is bacterial nitric oxide reductase (NOR),² which catalyzes two-electron reduction of NO to N₂O, a crucial step in the denitrification pathway.³ Since no 3D structure is available, bioinformatic studies suggest that NOR shares similar structural features as heme-copper oxidases (HCOs) whose structures are available.⁴ Both NOR and HCO contain a heme b₃ and a 3-histidine (His) metal center, with the metal site occupied by a nonheme iron in NOR (called Fe_B) and a copper in HCOs (called Cu_B). Computational modeling also indicates one or two glutamates (Glu) are close to the Fe_B site,⁵ which are essential for NOR activity.⁶ However, whether the Glu serves as a ligand to Fe_B remains uncertain. Recently, we have rationally designed a structural and functional NOR by construction of a 3-His-1-Glu

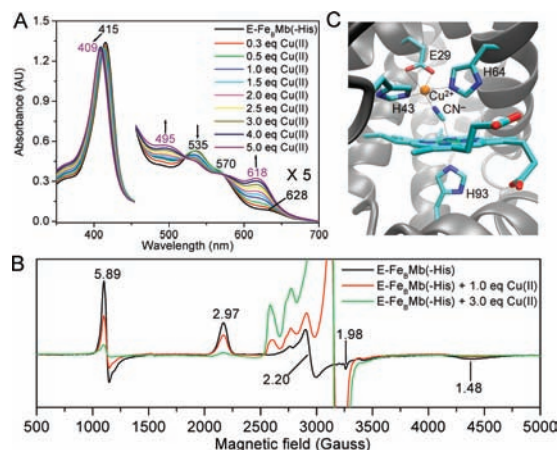


Figure 1. (A) UV-vis titration of ferric E-Fe_BMb(-His) with Cu(II) in 25 mM KH₂PO₄, 75 mM KCl, pH 7.0, 25 °C. (B) X-band EPR spectra of ferric E-Fe_BMb(-His) (0.5 mM) in the same buffer as in (A) and that in the presence of 1.0 or 3.0 equiv of Cu(II). The spectra were collected at 20 K, 5 mW power, and 9.05 GHz. (C) Crystal structure of Cu(II)-CN⁻-Fe_BMb(-His) at 1.65 Å resolution (PDB entry 3MN0).

Fe_B center in sperm whale myoglobin (swMb), called Fe_BMb (swMb L29H, F43H, H64, V68E), and demonstrated that both His and Glu ligands are essential for iron binding and NO reduction activity.^{2a}

While it is exciting to find that the 3-His-1-Glu Fe_B center can bind iron and confer NOR activity, a recent sequence alignment has predicted that a unique quinone-oxidizing NOR, gNOR, may exhibit a novel Fe_B site, with one of the 3-His ligands replaced by an Asp residue, although the exact structure is not available.⁷ This finding is quite interesting, as an inspection of the active site of nonheme iron containing enzymes in nature indicates that the majority use a similar conserved 2-His-1-carboxylate (Asp/Glu) facial triad for iron binding and substrate oxidation.⁸ To test whether the unique 2-His-1-Asp/Glu nonheme metal center could be utilized to mimic NOR for NO reduction, we herein report introduction of a 2-His-1-Glu metal center in swMb by replacing His29 in Fe_BMb with a Glu residue while keeping Val68 intact (Fe_BMb H29E, E68 V, or swMb L29E, F43H, H64, called Fe_BMb(-His)). As designed and demonstrated, Fe_BMb(-His) can bind iron and copper, with both proteins displaying NOR activity.

The Fe_BMb(-His) was prepared using a protocol described previously.^{2,9} As isolated, it displays a red color, with a Soret band at 415 nm and visible absorptions at 535 and 570 nm (Figure 1A), resembling those of metMb in the presence of imidazole.¹⁰ The EPR spectrum exhibits signals at *g* = 2.97, 2.20, and 1.48 (Figure 1B), typical of a low-spin ferric heme and similar to those of the

[†] Department of Chemistry, University of Illinois at Urbana–Champaign.

[‡] George L. Clark X-ray Facility & 3M Materials Lab, University of Illinois at Urbana–Champaign.

[§] Department of Biochemistry, University of Illinois at Urbana–Champaign.

^{||} Brookhaven National Laboratory.

^{*} Present address: School of Chemistry of Chemical Engineering, University of South China, Hengyang 421001, China.

heme *b* with bis-histidine ligation in NOR ($g = 2.96, 2.26, \text{ and } 1.46$).¹¹ In addition, minor high-spin heme signals at $g = 5.89$ and 1.98 were observed, in agreement with the UV-vis spectrum that shows a small charge-transfer band at 628 nm. Addition of Cu^{2+} to oxidized protein that contains ferric heme, but no metal ion in the Fe_B site (called ferric E- $\text{Fe}_B\text{Mb}(-\text{His})$), resulted in a shift of the Soret band from 415 to 409 nm, a decrease of 535 nm absorption, and concomitant increase of the 495 and 618 nm bands. The resultant new spectrum (409, 495, and 618 nm) is characteristic of a high-spin ferric heme, suggesting that one of the ligands dissociates from the heme iron and coordinates to copper, causing a low-spin to high-spin heme transition. This conclusion was further supported by EPR spectroscopy (Figure 1B); the low-spin signal at $g = 2.97$ decreased upon Cu^{2+} addition. Instead of an increase of the high-spin signal at $g = 5.89$, as predicted by UV-vis spectra, the high-spin signal decreased, most likely due to spin coupling between heme- $\text{Fe}(\text{III})$ and $\text{Cu}(\text{II})$.¹² To support this interpretation, addition of Zn^{2+} , a metal ion with no unpaired electrons, produced an increase in the high-spin signals and a decrease in the low-spin signals (Figure S1). Furthermore, titration of ferric E- $\text{Fe}_B\text{Mb}(-\text{His})$ with $\text{Cu}(\text{II})$ in the presence of cyanide results in a shift in the Soret band to 421 nm (Figure S2) due to the formation of a heme- $\text{Fe}(\text{III})\text{-CN}^-$ - $\text{Cu}(\text{II})$ bridge, as evidenced by a high resolution crystal structure (Figure 1C, Table S1). In the structure, two His and one Glu coordinate to $\text{Cu}(\text{II})$ (2.27 Å to H43, 2.30 Å to H64, and 2.25 Å to E29) with the N atom of CN^- (1.83 Å) making up the fourth coordination. A weak interaction with the other O atom of E29 (3.01 Å) also exists. These results demonstrate that a unique 2-His-1-Glu metal center was successfully created in swMb.

The UV-vis spectrum of deoxy E- $\text{Fe}_B\text{Mb}(-\text{His})$ (Soret, 432 nm; visible, 556 nm, Figure S3) is characteristic of a five-coordinate ferrous heme, indicating a conformation change upon heme reduction. In the presence of $\text{Cu}(\text{I})$, $\text{Fe}(\text{II})$, or $\text{Zn}(\text{II})$, the Soret and visible bands decrease slightly in intensity, providing evidence of metal binding (Figure S3). In addition, nitric oxide readily binds to deoxy E- $\text{Fe}_B\text{Mb}(-\text{His})$, resulting in new peaks at 419, 545, and 578 nm (Figure S4). The complex of deoxy E- $\text{Fe}_B\text{Mb}(-\text{His})\text{-NO}$ is stable without metal or with $\text{Zn}(\text{II})$ in the Fe_B site. However, the Soret band of $\text{Cu}(\text{I})\text{-Fe}_B\text{Mb}(-\text{His})\text{-NO}$ was found to be 400 nm, which becomes more intense and is red-shifted to 416 nm after ~1 h. This observation is in contrast to $\text{Fe}(\text{II})\text{-Fe}_B\text{Mb}(-\text{His})\text{-NO}$, in which the Soret band decreases and is blue-shifted from 419 to 416 nm (Figure S5). Note that the resultant spectrum in both cases is similar to that of ferric E- $\text{Fe}_B\text{Mb}(-\text{His})$ in the presence of NO (Figure S4B). These observations provide valuable evidence of NO reduction activity for both $\text{Cu}(\text{I})\text{-Fe}_B\text{Mb}(-\text{His})$ and $\text{Fe}(\text{II})\text{-Fe}_B\text{Mb}(-\text{His})$. The two electrons required for the reduction of NO to N_2O come from the reduced heme iron and from either $\text{Cu}(\text{I})$ or $\text{Fe}(\text{II})$. After NO reduction, the heme returns to a ferric state, mimicking one turnover conditions. In addition, the contrasting spectral changes observed suggest that different intermediates occur during NO reduction, depending on which metal is in the nonheme Fe_B site ($\text{Cu}(\text{I})$ or $\text{Fe}(\text{II})$).

To provide more information about the intermediates, the NO reduction process was monitored by EPR. As shown in Figure 2, the spectrum of E- $\text{Fe}_B\text{Mb}(-\text{His})\text{-NO}$ is typical of a six-coordinate low-spin heme-NO species with 9-line hyperfine splitting resulting from both the bound NO and the proximal histidine.¹³ In the presence of $\text{Cu}(\text{I})$, the hyperfine splitting decreases after 1 min of incubation with NO, which is likely due to a weakening of the proximal histidine bond to the heme iron.¹⁴ After 5 min, a 3-line hyperfine structure appears that is characteristic of a five-coordinate heme-NO species, indicating that the proximal heme Fe-His bond

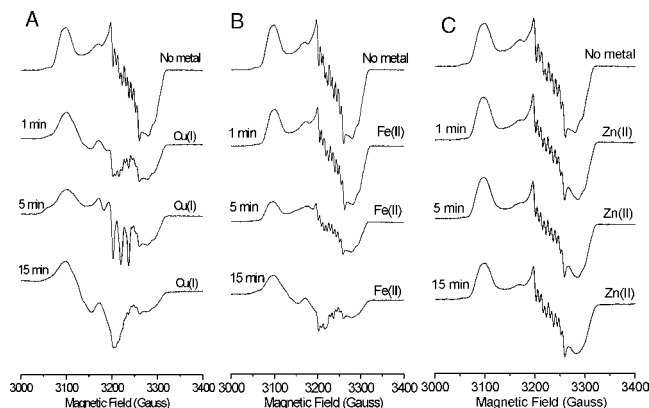


Figure 2. EPR spectra of deoxy E- $\text{Fe}_B\text{Mb}(-\text{His})$ (0.5 mM) in the presence of NO after 5 min (top line), with 2 equiv of $\text{Cu}(\text{I})$ (A), $\text{Fe}(\text{II})$ (B) or $\text{Zn}(\text{II})$ (C) incubated with NO for 1 min, 5 min, and 15 min. Spectra were collected in 50 mM Bis-Tris pH 7.0 at 30 K, 0.2 mW power, and 9.05 GHz.

is broken.¹³ In contrast, this spectral change was not observed for $\text{Cu}(\text{I})\text{-Cu}_B\text{Mb-NO}$ that has a 3-His metal center (H29, H43, and H64),¹⁴ indicating that Glu29 plays a crucial role in forming a five-coordinate heme intermediate. At longer time points, the hyperfine splitting evolved into a broad peak, likely due to the reduction of NO and oxidation of $\text{Fe}_B\text{Mb}(-\text{His})$. Note that both $\text{Cu}(\text{II})\text{-NO}$ ¹⁵ and six-coordinate ferric heme- NO ^{1b} complexes are EPR silent, probably due to antiferromagnetic coupling between the unpaired electron on NO and that in $\text{Cu}(\text{II})$ or ferric heme. On the other hand, for $\text{Fe}(\text{II})\text{-Fe}_B\text{Mb}(-\text{His})\text{-NO}$, only slight signal decreases were observed up to 5 min. At 15 min, similar to that of $\text{Cu}(\text{I})\text{-Fe}_B\text{Mb}(-\text{His})\text{-NO}$ at 1 min, the hyperfine splitting decreased, suggesting the heme Fe-His bond was weakened, but not cleaved. In the case of redox-inactive $\text{Zn}(\text{II})$, no spectral changes were observed for $\text{Zn}(\text{II})\text{-Fe}_B\text{Mb}(-\text{His})\text{-NO}$. Interestingly, a five-coordinate heme-NO species has been observed for both NOR^{11,16} and the member of the HCO family with the highest NO reduction activity, cytochrome *cbh3* oxidases.¹⁷ However, in our case, this five-coordinate species was detected only for $\text{Cu}(\text{I})\text{-Fe}_B\text{Mb}(-\text{His})$, not for $\text{Fe}(\text{II})\text{-Fe}_B\text{Mb}(-\text{His})$ or $\text{Zn}(\text{II})\text{-Fe}_B\text{Mb}(-\text{His})$. These observations suggest that not only the ligand, as in Glu29, but also the identity of the metal in the nonheme center play crucial roles in determining the nature of the intermediate.

To confirm the product of NO reduction, GC/MS was carried out under single turnover conditions by monitoring N_2O formation in the head space of the solution (Figure S6). When $\text{Cu}(\text{I})\text{-Fe}_B\text{Mb}(-\text{His})$ was exposed to excess NO, N_2O could be observed to form with increased yield over time as estimated from the ratio of N_2O :NO peaks (~32% at 20 h). N_2O production was also observed for $\text{Fe}(\text{II})\text{-Fe}_B\text{Mb}(-\text{His})$ (~6% at 20 h). In contrast, no N_2O formation was observed for $\text{Zn}(\text{II})\text{-Fe}_B\text{Mb}(-\text{His})$, metal alone, and wtMb with $\text{Cu}(\text{I})$ ¹⁴ or with $\text{Fe}(\text{II})$.^{2a} These results demonstrate that $\text{Cu}(\text{I})$ or $\text{Fe}(\text{II})$ in the Fe_B site plays a vital role in NO reduction. Note that because of the high solubility of N_2O (~25 mM in water at room temperature), GC/MS cannot be used to quantify the rates of NO reduction in the head space under these conditions. The relative activities of $\text{Cu}(\text{I})\text{-Fe}_B\text{Mb}(-\text{His})$ and $\text{Fe}(\text{II})\text{-Fe}_B\text{Mb}(-\text{His})$ are likely closely associated with the intermediates formed during NO reduction, with a five-coordinate heme intermediate leading to high NOR activity.^{2b,11,16,17}

In summary, the 2-His-1-Glu metal center commonly found in natural nonheme iron enzymes was engineered into myoglobin, and this new protein is capable of binding both $\text{Cu}(\text{I})$ or $\text{Fe}(\text{II})$ in the designed nonheme Fe_B site and of reducing NO to N_2O via different intermediates. This study thus presents a novel structural and

functional protein model of NOR and provides insights into the newly discovered member of the NOR family, gNOR.

Acknowledgment. We thank Dr. Mark J. Nilges for help with EPR analysis, Furong Sun and Beth D. Eves for aiding in GC/MS data collection, and Dr. James Hemp for discussions regarding gNOR. This work was supported by the NIH Grant GM062211.

Supporting Information Available: Complete ref 7, experimental details, EPR for Zn(II) binding, UV-vis and GC/MS for NO reduction, and X-ray crystallographic data. This material is available free of charge via the Internet at <http://pubs.acs.org>.

References

- (1) (a) Lu, Y.; Yeung, N.; Sieracki, N.; Marshall, N. M. *Nature* **2009**, *460*, 855–862. (b) Collman, J. P.; Yang, Y.; Dey, A.; Decréau, R. A.; Ghosh, S.; Ohta, T.; Solomon, E. I. *Proc. Natl. Acad. Sci. U.S.A.* **2008**, *105*, 15660–15665. (c) Kaplan, J.; DeGrado, W. F. *Proc. Natl. Acad. Sci. U.S.A.* **2004**, *101*, 11566–11570. (d) Wasser, I. M.; de Vries, S.; Moënné-Loccoz, P.; Schröder, I.; Karlin, K. D. *Chem. Rev.* **2002**, *102*, 1201–1234.
- (2) (a) Yeung, N.; Lin, Y.-W.; Gao, Y.-G.; Zhao, X.; Russell, B. S.; Lei, L.; Miner, K. D.; Robinson, H.; Lu, Y. *Nature* **2009**, *462*, 1079–1082. (b) Lin, Y.-W.; Yeung, N.; Gao, Y.-G.; Miner, K. D.; Tian, S.; Robinson, H.; Lu, Y. *Proc. Natl. Acad. Sci. U.S.A.* **2010**, *107*, 8581–8586.
- (3) Watmough, N. J.; Field, S. J.; Hughes, R. J. L.; Richardson, D. J. *Biochem. Soc. Trans.* **2009**, *37*, 392–399.
- (4) Ji, H.; Das, T. K.; Puustinen, A.; Wikström, M.; Yeh, S.; Rousseau, D. L. *J. Inorg. Biochem.* **2010**, *104*, 318–323.
- (5) Reimann, J.; Flock, U.; Lepp, H.; Honigsmann, A.; Ädelroth, P. *Biochim. Biophys. Acta* **2007**, *1767*, 362–373.
- (6) Butland, G.; Spiro, S.; Watmough, N. J.; Richardson, D. J. *J. Bacteriol.* **2001**, *183*, 189–199.
- (7) Sievert, S. M.; et al. *Appl. Environ. Microbiol.* **2008**, *74*, 1145–1156.
- (8) (a) Kovaleva, E. G.; Lipscomb, J. D. *Nat. Chem. Biol.* **2008**, *4*, 186–193. (b) Tshuva, E. Y.; Lippard, S. J. *Chem. Rev.* **2004**, *104*, 987–1011.
- (9) (a) Sigman, J. A.; Kwok, B. C.; Lu, Y. *J. Am. Chem. Soc.* **2000**, *122*, 8192–8196. (b) Sigman, J. A.; Kim, H. K.; Zhao, X.; Carey, J. R.; Lu, Y. *Proc. Natl. Acad. Sci. U.S.A.* **2003**, *100*, 3629–3634.
- (10) Diven, W. F.; Goldsack, D. E.; Alberty, R. A. *J. Biol. Chem.* **1965**, *240*, 2437–2441.
- (11) Sakurai, T.; Sakurai, N.; Matsumoto, H.; Hirota, S.; Yamauchi, O. *Biochem. Biophys. Res. Commun.* **1998**, *251*, 248–251.
- (12) Cheesman, M. R.; Oganessian, V. S.; Watmough, N. J.; Butler, C. S.; Thomson, A. J. *J. Am. Chem. Soc.* **2004**, *126*, 4157–4166.
- (13) Decatur, S. M.; Franzen, S.; DePillis, G. D.; Dyer, R. B.; Woodruff, W. H.; Boxer, S. G. *Biochemistry* **1996**, *35*, 4939–4944.
- (14) Zhao, X.; Yeung, N.; Russell, B. S.; Garner, D. K.; Lu, Y. *J. Am. Chem. Soc.* **2006**, *128*, 6766–6767.
- (15) Sarma, M.; Kalita, A.; Kumar, P.; Singh, A.; Mondal, B. *J. Am. Chem. Soc.* **2010**, *132*, 7846–7847.
- (16) Kumita, H.; Matsuura, K.; Hino, T.; Takahashi, S.; Hori, H.; Fukumori, Y.; Morishima, I.; Shiro, Y. *J. Biol. Chem.* **2004**, *279*, 55247–55254.
- (17) Pinakoulaki, E.; Stavarakis, S.; Urbani, A.; Varotsis, C. *J. Am. Chem. Soc.* **2002**, *124*, 9378–9379.

JA103516N